

Asking ‘which is real?’ to refute symmetries

Rupert Tombs and Christopher G. Lester

November 2021

Abstract

Which of m and \mathfrak{m} is a real letter? If you know, then their printing is not symmetric. Interesting physical models often imply symmetries, and experiments often have symmetrical designs. Theoretical models are imperfect, and engineering is not infinitely precise; both cases demand practical methods which challenge symmetries by inspecting data. Critically, such methods must handle filtered data, which commonly arises from inefficiencies, blind-spots or deliberate selections, and might give the illusion of asymmetry if mistreated. We construct such a method in this paper, which uses generic machine learning algorithms to train models which predict *which is real* between observed data and symmetrically transformed clones. If they predict accurately in independent tests, then the symmetry is violated. We use examples to demonstrate how the method works and how the models’ predictions can be interpreted.

1 Introduction

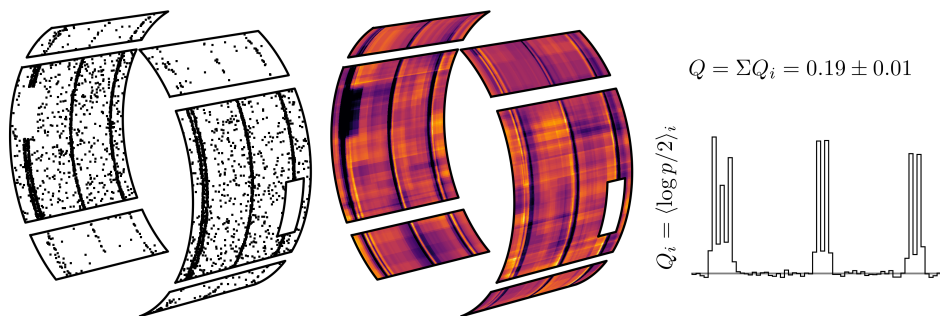


Figure 1: (left) Training data are shown on a gappy cylindrical detector; the smaller panels filter 90% of data in their space; gaps detect no data. (middle) A learned function predicts that data in yellow areas as more likely to be real than versions in the dark purple regions; it finds a missing patch and an offset which varies with angle. (right) Positive Q refutes rotational symmetry; the histogram shows contributions to this evidence from circumferences along the length.

What If nature refutes a symmetry, then all models which imply that symmetry are wrong. Common contexts do imply symmetries, perhaps from theoretical hypothesis or hardware design, and we aim to challenge those symmetries in a general way by testing them in data.

Real data are messy. Not only do data take complicated shapes, they are usually subject to lossy effects in collection and processing. However, inefficiencies are often well understood, and select subsets of the data can have cleaner connections to their idealized modelling; to work in practice, it is critical that our method works seamlessly in the presence of such filtering or selections of the data.

How If a symmetry is respected, then each data point has symmetrically equivalent fake cousins which, given all other observed information, cannot be distinguished. Between pairs of these symmetrically equivalent data, one real and one fake, one cannot know ‘which is real?’, but can at best assign equal probability to each. This statement is key to our method.

For our purposes, a model is a rule which assigns probabilities. Symmetry is a model because it assigns equal probabilities. Asymmetry is not a model because it is ambiguous; there are innumerable many asymmetric models, so we can only explore examples.

Where an asymmetric model consistently succeeds in identifying real data from transformed fakes, the symmetry must be violated. We attempt this refutation by using general-purpose machine learning algorithms to train promising asymmetric models, then testing those models’ predictions.

The method requires numerical data, a way to transform them under the candidate symmetry subject to filtering, and an appropriate learning algorithm to assign the asymmetric model.

With finite data the results are not certain, but testing on independent datasets does give cleanly interpretable results which can usefully guide further investigations.

Context This is an example of self-supervised learning, in which models are trained via auxiliary tasks to understand structures in the data without external labelling, such that other objectives are learned more efficiently [1–6]. Our emphasis is not on the training, however, but on the models’ performance with the self-supervised task itself.

Active research pursues ways to build symmetries into machine learning algorithms [7–10], with scientific applications including high energy physics [11–13] and astronomy [14, 15]. These are useful ways to encode domain-specific prior information, which improves performance by leaving less to learn from data. In contrast, we seek to challenge those priors in contexts where they may or may not hold.

The methods constructed here are a probabilistic recasting of those developed in our sister paper at Reference [13]. We informally discuss various mathematical properties of symmetries which are formalized in another sibling at Reference [16].

Layout Before fully introducing the ‘which is real?’ method, we use Section 2 to describe a simpler ‘is it real?’ method which does not quite meet our needs; ‘is it real?’ uses a standard classification setup in which models predict labels in a mixed dataset, but it struggles to handle filtered data and has some inelegance in how to construct its mixed data. How ‘which is real?’ works to resolve these issues is described in Section 3. We then study examples, beginning with the cylindrical detector from Figure 1 in Section 4 and a map with less trivial symmetry in Section 5.

2 Is it real?

For ‘is it real?’, a dataset is prepared with the two classes: real and fake; the fakes are transformed clones of real data which would be symmetrically equivalent if the symmetry were respected.

Transitions For symmetries with many equivalent states it is impractical to make all possible fakes. But there is no need to; examples can be sufficient. To be general, we sample fakes with a probability distribution $d\tau(x' | x)$ which takes a data entry x to hypothetically equivalent states x' . We are interested in symmetries of data distributions themselves, so this should apply prior to any filtering, which is discussed below. For now, the transition distribution $d\tau(x' | x)$ is relatively unconstrained; it may not support all equivalent states and could even map each x to a deterministic output $x' = t(x)$. The choice of transitions determines which opportunities there are to find asymmetry, and may be influenced by practical considerations.

For the methods discussed here, transition distributions are the mechanism by which the target symmetries are encoded.

Data preparation To apply the ‘is it real?’ method, a mixed dataset should be prepared with equal proportions of real and fake data shuffled together. To finish describing the remainder of this method, we briefly defer discussion of how the data, transition distribution and filter can combine to achieve this preparation.

With a mixed dataset prepared, standard machine learning practice can be applied: train an asymmetric classification model to predict the real–fake label of one part of the dataset, and test its predictions on another. We want to compare this candidate asymmetric model against the symmetric model which, since the real and fake data distributions are constructed to be symmetrically equivalent, can only assign probability $1/2$ to each class.

Quality Data contributes to model comparison through likelihoods, which are the probabilities assigned to the data by the models. Our likelihood is a product over the independent predictions, but to have a quantity which converges a fixed value as the number of data n increases, we define a quality function as the mean log likelihood ratio

$$Q(\{\ell\}, \{x\}, p) = \frac{1}{n} \sum_{i=1}^n \log p(\ell_i | x_i) - \log \frac{1}{2} \quad (1)$$

for labels $\ell_i \in \{\text{real}, \text{fake}\}$ and label probabilities $p(\ell_i | x_i)$ assigned by the learned model. This may be recognised as a difference of binary cross-entropies, and is invertible to the likelihood if n is known. This Q has a maximum value of $\log(2) \approx 0.69$ for perfect predictions, but is not bounded from below.

Since a model is fixed when predicting elements of the test set, the terms of this sum are independent and standard estimation methods can be applied assign reasonable uncertainties to its limiting value, which is the expectation value of the log likelihood ratio.

If Q is significantly greater than zero, then the model is predicting more accurately than symmetry would allow, which indicates that the symmetry is violated. If symmetry is preserved, then Q is expected to be less than zero since learning algorithms are unlikely to find the exact $p = 1/2$ solution.

Filtering and other problems We now return to the mixed dataset. It is unusual for all possible data to be recorded, due to the holes, imperfections or selections which can be thought of as filtering the data before observation. We describe these effects with a filter function $L(x)$ which assigns a probability that a data point x is received; for an unreliable sensor it might be $L(x) = 0.1$, and for hard removal it would be zero.

We are interested in symmetries of data distributions and not of filters. Fakes should therefore be sampled as if pure data were collected, resampled from $d\tau(x' | x)$, and then filtered by $L(x)$. However, real data have already been filtered, and so the pre-filtering data distribution is related through division by the filter function. Applying these relations, the distribution of fakes can be written

$$dp(x' | \text{fake}) = \int \left[\frac{L(x')}{L(x)} d\tau(x' | x) \right] dp(x | \text{real}). \quad (2)$$

When $dp(x | \text{real})$ is approximated by an ensemble of real data, this means that each data entry is weighted by a ratio of filters. Although $L(x)$ cannot be zero for observed data, we do have a problem when $L(x) \ll L(x')$; such data which pass tight filtering require many faked copies, which in extreme cases could come to dominate the estimated fake distribution, giving an unappealing imbalance.

Weights on real data also mean that the frequency with which each entry should be chosen to transform to a fake depends upon all other data, and may change drastically as highly-weighted data are observed. In fact, this problem exists without weights; the strategy of mixing all transformed data together raises questions about how the fake examples should be constructed.

Which data should be used to approximate $dp(x | \text{real})$ when generating fakes? If only the training set is used, then a sufficiently advanced model could memorize those examples and recognise different test data as real. If both training and testing sets are used, then testing information leaks into training and the label prediction again reduces to memory. If testing examples are incrementally included after their labels are predicted, then the testing scores depend upon which were previously seen, breaking the independence which is so useful to their interpretation.

With large data sets for which only batched analysis is practical due to limited computer memory, the dependence on a large ensemble of examples to generate fakes becomes a problem in itself.

None of these issues kills ‘is it real?’ the method outright (especially if allowing a reasonable degree of approximation) but they do make it inelegant; ‘is it real?’ can work, but we would prefer a method which does not require division by the filter function, and in which the entries are treated with independence.

Although weights due to filtering and dependence are problems, there is also opportunity in the freedom to choose transition distributions $d\tau(x' | x)$. The ‘which is real?’ method avoids these problems while restricting that freedom.

3 Which is real?

The ‘which is real?’ method tests symmetries by attempting to discriminate each data entry from an augmented clone of itself; since each data entry is treated alone, the independence issue is resolved immediately. With filtering, data weights are also avoided by not attempting to undo the filter, but by applying it a second time when sampling each fake.

Again, a transition distribution $d\tau(x' | x)$ is used to sample fakes, and in doing so defines the candidate symmetry. Given an x - x' pair, we have two class labels

corresponding to its two orderings: real–fake (x is real and was transformed to x' ; $x' \leftarrow x$) and fake–real (x' is real and was transformed to x ; $x \leftarrow x'$).

The classification problem is now to predict which of fake–real and real–fake labels is correct, and it could be naïvely approached by learning a label probability on the joint x – x' space. However, that would mean working with an input space twice as large as the original data, and this incurs costs in learning performance and interpretability when inspecting outputs. Thankfully, this problem is avoidable; classification can be reduced to learning a function on the original data space, with the difference of its values at both x and x' used to assign probabilities.

Classification To explain, we need a little theory. Binary classification can be expressed as estimating an odds ratio between distributions, which is conveniently handled as its logarithm:

$$\phi(x, x') = \log \frac{dp(x' \leftarrow x)}{dp(x \leftarrow x')} = \log \frac{d\tau(x' | x)dp(x)}{d\tau(x | x')dp(x')}, \quad (3)$$

in which the rightmost expression factors the input construction into the steps of real data being received, then fakes being sampled by transitioning from them.

This log odds simplifies if we require that the transition distribution is symmetrical under exchange of its arguments: $d\tau(x' | x) = d\tau(x | x')$ for all accessible x – x' pairs. Then the transition terms cancel and $\phi(x, x')$ becomes a difference of two terms:

$$\phi(x, x') = \log \frac{dp(x)}{dp(x')} = \zeta(x) - \zeta(x'), \quad (4)$$

where $\zeta(x)$ is suitable for learning since it is unbounded and real-valued. Learning $\zeta(x)$ does not correspond exactly to learning the data distribution, but only a relative density with respect to an unspecified measure $\mu(x)$, since $\zeta(x) = \log(dp/d\mu)(x)$ is a solution for any μ which supports p .

From these objects, label probabilities are related through the logistic function:

$$p(\text{real-fake} | x, x') = \frac{1}{1 + e^{-\phi(x, x')}} = \frac{1}{1 + e^{-(\zeta(x) - \zeta(x'))}}. \quad (5)$$

Properties Not only does this separation halve the size of the input space, the construction as a difference ensures that $\phi(x, x')$ is correctly antisymmetric under exchange of its arguments. This means there is no difference between x – x' labelled real–fake and x' – x labelled fake–real, and there is no need to shuffle the ordering, as would be needed to learn a naïve $\phi(x, x')$. We can choose to always order the data real–fake.

Symmetrical transitions mean that space is partitioned into one or more disjoint sets of data within which all data are connected through $d\tau(x' | x)$. We call these sets orbits. Within each orbit, the assigned probabilities are unaffected by additive shifts in $\zeta(x)$, and such shifts can vary arbitrarily between orbits; this freedom is granted to the learning algorithm, and means that some care is required when interpreting the modelled $\zeta(x)$.

Transitions and filtering Although transition symmetry is a stronger constraint than was required for ‘is it real?’, the constraint is not too stringent; it is generally satisfied by setting $d\tau(x' | x)$ to the probability distribution which is invariant under the action of the symmetry.¹ Some symmetries have no such probability distribution,

¹The transition from x to itself may be excluded to avoid wasted comparisons.

however. For example, translation invariance on the real line would require a uniform-everywhere distribution which cannot be normalized.

In practice, such distributions must be normalizable after filtering since real data are measured and recorded with finite instruments. We can therefore safely assume that a satisfactory transition distribution by is made scaling the symmetry-invariant measure by the filter function.

With a filter function $L(x)$ applied to both real and fake data, then all four of its instances cancel from the log odds and leave it unchanged;

$$\phi(x, x') = \log \frac{L(x')d\tau(x' | x)L(x)dp(x)}{L(x)d\tau(x | x')L(x')dp(x')} = \log \frac{dp(x)}{dp(x')}. \quad (6)$$

The same $\zeta(x)$ construction can be applied, and successful learning algorithms should approach the unfiltered result wherever they receive enough data.

Wrap-up Symmetry testing for ‘which is real?’ works as for ‘is it real?’: train with one portion of the data and test on another by evaluating Q according to Equation 1.

Each data entry is now compared to a faked version of itself, which should be sampled according to the product of a symmetric transition distribution and any filter function through which the data have already passed.

Training learns a function $\zeta(x)$, from which differences assign real–fake odds which translate to label probabilities through the logistic function. The product of those probabilities gives a differentiable likelihood function for use in training.

Extensions The basic method described here is open to some extensions. While it was described with only one fake per data entry, more can be used by averaging their log probabilities in the sum for Q . Multiple repeats may help or hinder training, but can be implemented efficiently since $\zeta(x)$ need only be evaluated once for the real entry and once for each fake.

We have made minimal references to the learning algorithms’ details since they are irrelevant to the method itself. In any application, it is the task of a user to find and apply a practical approach.

The following examples exercise all parts of the ‘which is real?’ method while attempt to include much of the complexity of real data. With their relatively simple data, standard machine learning tools are found to perform well with minimal parameter tuning.

4 Example 1: Cylindrical detector

The broken ring shown in Figure 1 illustrates an imaginary detector which is used to measure point data on its surface. These data could for example represent estimates of where energetic particles interacted with its surface, but the application is free. The leftmost plot of this figure shows the training set of five thousand data at their measured locations.

To demonstrate data filtering, the smaller panels are imagined to be made from thin materials which miss 90% of possible data, and the illustrated gaps between (and in) those sensitive detectors do not record anything. The filter function is therefore $L(x) = 1$ for x in a large panel, $L(x) = 0.1$ for x in a small panel, and $L(x) = 0$ otherwise.

The candidate symmetry is of rotation about the axis of the cylinder. Each data point is specified by its longitudinal position z and its angle ϕ , so the transformation distribution $d\tau(x' | x)$ is uniform for ϕ between 0 and 2π .

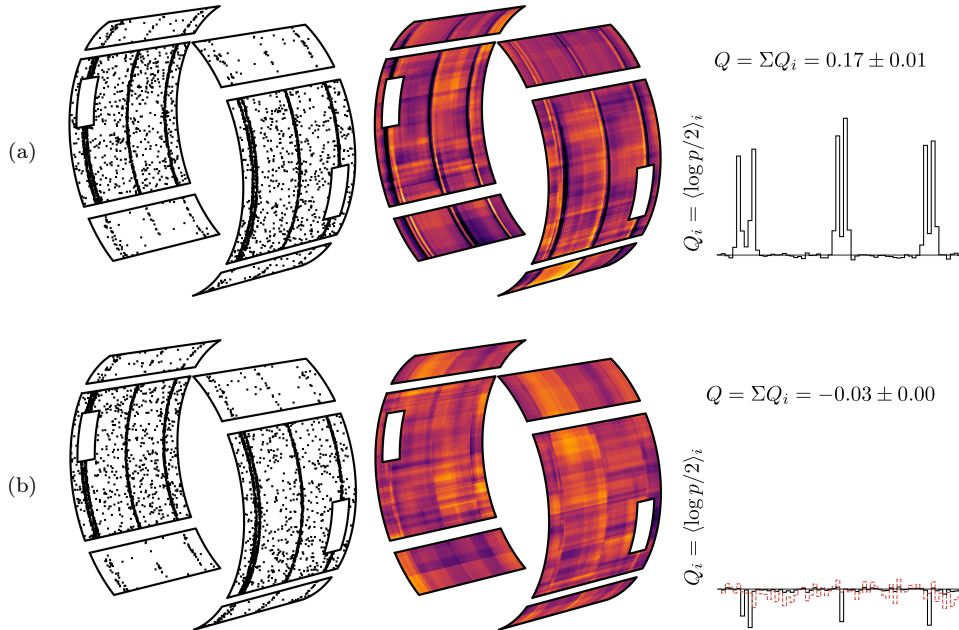


Figure 2: Modifications to the gappy cylindrical detector from Figure 1. (a) The hole in the back panel is included in filter function, weakening the observed asymmetry. (b) The sinusoidal offset is removed and fresh data are sampled. The asymmetric model does worse than the symmetric model because it assigns non-1/2 probabilities to data from a symmetric distribution. Since the Q_i bins are summed totals, the negative spikes show where data are denser; the dashed orange line shows the mean in each bin times 100, demonstrating that the model does not perform worse on average in those spikes. More details are given in the text of Section 4.

For a model training, we use LightGBM [17] as a fast and robust algorithm which works with minimal tuning. Like other boosted decision tree models [18], its output $\zeta(x)$ is a weighted sum of step functions acting on a tree of inequalities on the data features; these step functions' locations and weights are learned from the first two derivatives of a loss function with respect to the model outputs. Our loss is the negative sum of the log likelihoods from Equation 5, whose derivatives with respect to $\zeta(x)$ and $\zeta(x')$ are readily computed.

A $\zeta(x)$ function learned by LightGBM² is displayed in the middle plot of Figure 1; its colour map is clipped to the range from -2 (black) to $+2$ (bright yellow). A large purple hole has appeared where training data are lacking; the model knows that any data seen there are probably fake, having been rotated in from other angles. The circular stripes of high density are matched with purple and yellow fringes which swap sides between the two large panels; these correspond to an offset in z which varies sinusoidally with ϕ .

In the small panels, where data are sparse due to filtering, $\zeta(x)$ is somewhat smoother but shows similar structures to the main panels. Despite filtering, the algorithm is still learning towards the same underlying log odds, but does so with less

²This model uses default LightGBM 3.2.1 parameters through its scikit-learn interface [19,20], except for `subsample=0.5`, `subsample_freq=1`, and the custom 'which is real?' objective. Without subsampling the z coordinates, which are exactly repeated between data and fakes, appear to hinder training.

precision because it has fewer data.

The rightmost section of Figure 1 reports results from testing on five thousand independent data with one fake each. The histogram shows contributions to the Q sum, given in Equation 1, from bins along the z axis which accumulates contributions from orbits in ϕ . Positive bins on the edges of dense rings show that these locations have many data and that their fakes identify themselves due to the angular variation of ring offsets. The total $Q = 0.19 \pm 0.01$ is a strong indication that rotational symmetry is violated in these data (the quoted uncertainty is the standard deviation of the log likelihood sample divided by \sqrt{n}). Whether this asymmetry arises from the underlying physical process or experimental miscalibration is a matter for further investigation.

What happens when those asymmetric quirks are removed? Such changes are shown in Figure 2. Perhaps it is realized that the patch with no data in the back left panel is a gap in experimental hardware, much like the one on the front panel. Including that patch in the filter function with the same data results in the plots displayed in Figure 2a. This change correctly reduces the observed asymmetry, but otherwise has little effect on the $\zeta(x)$ surface.

Next, we remove the sinusoidally varying offset and sample new data from their new distribution. The result in Figure 2b shows no sign of asymmetry. In fact the true data distribution is symmetrical here, but the asymmetric model has not fully learned that from the finite training data; it therefore does worse than the symmetric model and receives a negative Q . The histogram on the right of this figure shows negative Q_i spikes at the dense rings; this is because those rings are dense, so have more data to add up. The average contribution in these regions is in fact closer to zero than elsewhere, as shown by the overlaid histogram.

5 Example 2: Height map

For circular symmetry and many others, symmetric transformations reduce to simply re-sampling one or more basic coordinates of x . This is not always the case; symmetries and their orbits may be non-trivial. To demonstrate this, we propose a symmetry around contours of constant height on a blocky topographical map, which is specified by the brightness of blobs in Figure 4. This symmetry states that the data density is translationally invariant within each connected region of constant colour on that map. The transition distribution from each data point is therefore uniform within its local blob.

Plausibly because observations are more sparse towards the edges of the map, the filter function removes 90% of data in a narrow bordering region, which is visible in the scatter plots of Figure 3. This figure contains examples with two different datasets, of which one obeys the symmetry and the other is augmented with waves which violate it. Again, LightGBM models³ are used with five thousand training data and five thousand testing data with one fake each. These waves show up in the learned $\zeta(x)$ function. Again the method successfully gives a significantly positive Q value only where the data are asymmetric, and the largest contributions to Q are attributable to orbits with many data and large asymmetry.

³These models use default LightGBM 3.2.1 parameters except for `max_depth=2` (to reduce overfitting) and the custom objective.

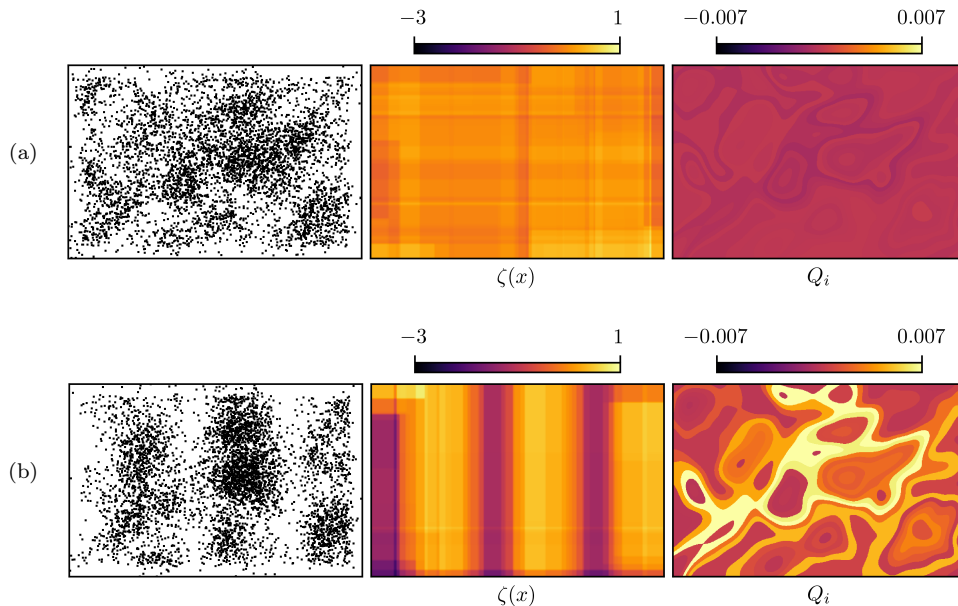


Figure 3: Applications of the ‘which is real?’ method with a candidate height map symmetry specified in Figure 4. Data in the visible bordering band pass the filter with probability 0.1. (a) Data density increases with map brightness and the symmetry is obeyed. For these symmetric data, $Q = -0.003 \pm 0.001$. (b) The data distribution is altered by waves with large amplitude. The model has learned these waves in its $\zeta(x)$ function, and contours which span these waves and have many data make the largest contributions to Q . For these asymmetric data, $Q = 0.060 \pm 0.004$. More details are given in the text of Section 5.

6 Conclusion

We propose the method of asking ‘which is real?’ between real and augmented data, and answering that question with probabilities assigned by flexible machine learning tools. This forms a general and practical method for challenging symmetries in data, which crucially works in the presence of selections and inefficiencies, collectively described as filtering. If the trained models answer successfully on independent data, then their probability assignments reveal where they have found asymmetry and indicate its scale. Success on non-trivial examples demonstrates that the method is ready to be exercised in real applications to test theoretically or experimentally proposed symmetries.

7 Acknowledgements

We thank Peterhouse for hosting and feeding this endeavour. RT thanks Daniel Noel for many useful questions and discussion, as well as Lars Henkelmann and other members of the Cambridge ATLAS machine learning discussion group, Homerton College, the Science and Technology Facilities Council, and the Cambridgeshire wind for blowing away distractions.

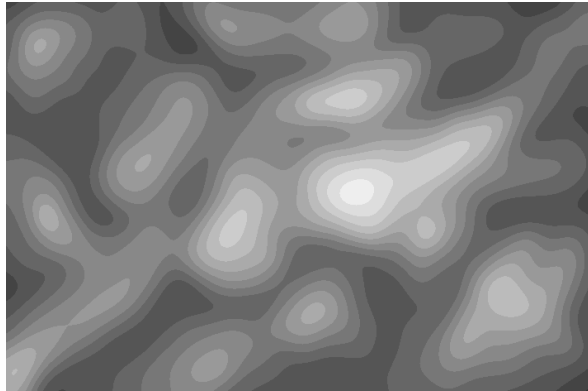


Figure 4: Symmetrical contours: the height map symmetry asserts that data density is uniform within each contiguous blob of constant brightness. That is, the terrain comprises discrete jumps and flat planes, as if it were made of stacked foam boards or voxels in a computer game. Data displayed in Figure 3 are sampled with density which increases with brightness.

References

- [1] Alexey Dosovitskiy, Jost Tobias Springenberg, Martin Riedmiller, and Thomas Brox. Discriminative unsupervised feature learning with convolutional neural networks. In Z. Ghahramani, M. Welling, C. Cortes, N. Lawrence, and K. Q. Weinberger, editors, *Advances in Neural Information Processing Systems*, volume 27. Curran Associates, Inc., 2014. URL: <https://proceedings.neurips.cc/paper/2014/file/07563a3fe3bbe7e3ba84431ad9d055af-Paper.pdf>.
- [2] Carl Doersch and Andrew Zisserman. Multi-task Self-Supervised Visual Learning. In *2017 IEEE International Conference on Computer Vision (ICCV)*, pages 2070–2079, 2017. doi:10.1109/ICCV.2017.226.
- [3] Aaron van den Oord, Yazhe Li, and Oriol Vinyals. Representation Learning with Contrastive Predictive Coding, 2019. arXiv:1807.03748.
- [4] Jacob Devlin, Ming-Wei Chang, Kenton Lee, and Kristina Toutanova. BERT: Pre-training of Deep Bidirectional Transformers for Language Understanding, 2019. arXiv:1810.04805.
- [5] Ting Chen, Simon Kornblith, Mohammad Norouzi, and Geoffrey Hinton. A simple framework for contrastive learning of visual representations. In *International conference on machine learning*, pages 1597–1607. PMLR, 2020.
- [6] Jean-Bastien Grill, Florian Strub, Florent Altché, Corentin Tallec, Pierre H. Richemond, Elena Buchatskaya, Carl Doersch, Bernardo Avila Pires, Zhaohan Daniel Guo, Mohammad Gheshlaghi Azar, Bilal Piot, Koray Kavukcuoglu, Rémi Munos, and Michal Valko. Bootstrap your own latent: A new approach to self-supervised Learning, 2020. arXiv:2006.07733.
- [7] Taco Cohen and Max Welling. Group Equivariant Convolutional Networks. In Maria Florina Balcan and Kilian Q. Weinberger, editors, *Proceedings of The 33rd International Conference on Machine Learning*, volume 48 of *Proceedings of*

- Machine Learning Research*, pages 2990–2999, New York, New York, USA, 20–22 Jun 2016. PMLR. URL: <https://proceedings.mlr.press/v48/cohenc16.html>.
- [8] Haggai Maron, Heli Ben-Hamu, Nadav Shamir, and Yaron Lipman. Invariant and Equivariant Graph Networks, 2019. [arXiv:1812.09902](https://arxiv.org/abs/1812.09902).
 - [9] Nathaniel Thomas, Tess Smidt, Steven Kearnes, Lusann Yang, Li Li, Kai Kohlhoff, and Patrick Riley. Tensor field networks: Rotation- and translation-equivariant neural networks for 3D point clouds, 2018. [arXiv:1802.08219](https://arxiv.org/abs/1802.08219).
 - [10] Marc Finzi, Max Welling, and Andrew Gordon Wilson. A practical method for constructing equivariant multilayer perceptrons for arbitrary matrix groups, 2021. [arXiv:2104.09459](https://arxiv.org/abs/2104.09459).
 - [11] HEP ML Community. A Living Review of Machine Learning for Particle Physics. URL: <https://iml-wg.github.io/HEPML-LivingReview/>.
 - [12] Alexander Shmakov, Michael James Fenton, Ta-Wei Ho, Shih-Chieh Hsu, Daniel Whiteson, and Pierre Baldi. Spanet: Generalized permutationless set assignment for particle physics using symmetry preserving attention, 2021. [arXiv:2106.03898](https://arxiv.org/abs/2106.03898).
 - [13] Christopher G. Lester and Rupert Tombs. Stressed GANs snag desserts, a.k.a Spotting Symmetry Violation with Symmetric Functions, 2021. [arXiv:2111.00616](https://arxiv.org/abs/2111.00616).
 - [14] Anna M M Scaife and Fiona Porter. Fanaroff–riley classification of radio galaxies using group-equivariant convolutional neural networks. *Monthly Notices of the Royal Astronomical Society*, 503(2):2369–2379, Feb 2021. URL: <http://dx.doi.org/10.1093/mnras/stab530>, doi:10.1093/mnras/stab530.
 - [15] Sander Dieleman, Kyle W. Willett, and Joni Dambre. Rotation-invariant convolutional neural networks for galaxy morphology prediction. *Monthly Notices of the Royal Astronomical Society*, 450(2):1441–1459, 04 2015. [arXiv:https://academic.oup.com/mnras/article-pdf/450/2/1441/3022697/stv632.pdf](https://academic.oup.com/mnras/article-pdf/450/2/1441/3022697/stv632.pdf), doi:10.1093/mnras/stv632.
 - [16] Christopher G. Lester. Chiral Measurements, 2021. [arXiv:2111.00623](https://arxiv.org/abs/2111.00623).
 - [17] Guolin Ke, Qi Meng, Thomas Finley, Taifeng Wang, Wei Chen, Weidong Ma, Qiwei Ye, and Tie-Yan Liu. LightGBM: A Highly Efficient Gradient Boosting Decision Tree. *Advances in neural information processing systems*, 30:3146–3154, 2017.
 - [18] Tianqi Chen and Carlos Guestrin. XGBoost: A Scalable Tree Boosting System. In *Proceedings of the 22nd acm sigkdd international conference on knowledge discovery and data mining*, pages 785–794, 2016.
 - [19] F. Pedregosa, G. Varoquaux, A. Gramfort, V. Michel, B. Thirion, O. Grisel, M. Blondel, P. Prettenhofer, R. Weiss, V. Dubourg, J. Vanderplas, A. Passos, D. Cournapeau, M. Brucher, M. Perrot, and E. Duchesnay. Scikit-learn: Machine Learning in Python. *Journal of Machine Learning Research*, 12:2825–2830, 2011.

- [20] Lars Buitinck, Gilles Louppe, Mathieu Blondel, Fabian Pedregosa, Andreas Mueller, Olivier Grisel, Vlad Niculae, Peter Prettenhofer, Alexandre Gramfort, Jaques Grobler, Robert Layton, Jake VanderPlas, Arnaud Joly, Brian Holt, and Gaël Varoquaux. API design for machine learning software: experiences from the scikit-learn project. In *ECML PKDD Workshop: Languages for Data Mining and Machine Learning*, pages 108–122, 2013.